Microlocal analysis of seven-dimensional Radon transforms for Compton scattering tomography

James Webber† and Todd Quinto*

Brigham and Women's Hospital† / Department of Mathematics, Tufts University*

Inverse Problems at a small scale, October 19, 2022

(Partial support from U.S. National Science Foundation, Simons Foundation)

Motivation

- Motivated by Compton Scattering Tomography (CST), we present a microlocal analysis of two novel Radon transforms which map functions to their integrals over apple and lemon surfaces.

Motivation

- Motivated by Compton Scattering Tomography (CST), we present a microlocal analysis of two novel Radon transforms which map functions to their integrals over apple and lemon surfaces.
- *Main applications:* Airport baggage and security screening, medical imaging.

Motivation

- Motivated by Compton Scattering Tomography (CST), we present a microlocal analysis of two novel Radon transforms which map functions to their integrals over apple and lemon surfaces.
- *Main applications:* Airport baggage and security screening, medical imaging.
- We consider the full 7-D manifold of apples and lemons and two natural submanifolds.

Motivation

- Motivated by Compton Scattering Tomography (CST), we present a microlocal analysis of two novel Radon transforms which map functions to their integrals over apple and lemon surfaces.
- *Main applications:* Airport baggage and security screening, medical imaging.
- We consider the full 7-D manifold of apples and lemons and two natural submanifolds.
- *Main goals:*
  - To understand when there are no microlocal artifacts (added singularities) in backprojections reconstructions from $R_j^* D \varphi R_j$.

Motivation

- Motivated by Compton Scattering Tomography (CST), we present a microlocal analysis of two novel Radon transforms which map functions to their integrals over apple and lemon surfaces.
- *Main applications:* Airport baggage and security screening, medical imaging.
- We consider the full 7-D manifold of apples and lemons and two natural submanifolds.
- *Main goals:*
  - To understand when there are no microlocal artifacts (added singularities) in backprojections reconstructions from $R_j^* D\varphi R_j$.
  - To predict and analyze the image artifacts with incomplete data.

Motivation

- Motivated by Compton Scattering Tomography (CST), we present a microlocal analysis of two novel Radon transforms which map functions to their integrals over apple and lemon surfaces.
- *Main applications:* Airport baggage and security screening, medical imaging.
- We consider the full 7-D manifold of apples and lemons and two natural submanifolds.
- *Main goals:*
  - To understand when there are no microlocal artifacts (added singularities) in backprojections reconstructions from $R_j^* D\varphi R_j$.
  - To predict and analyze the image artifacts with incomplete data.
  - To mitigate artifacts when possible.

The Compton Effect

The Compton effect determines scattering angle

E_{src}=energy of *monochromatic* photons at the source,

E_d=measured energy of scattered photon at detector,

E_0=electron rest energy, ω=scattering angle.

$$\frac{E_{\mathrm{src}} - E_d}{E_{\mathrm{src}}} = \frac{1 - \cos(\omega)}{E_0}$$

The Compton Effect

The Compton effect determines scattering angle

E_{src}=energy of *monochromatic* photons at the source,

E_d=measured energy of scattered photon at detector,

E_0=electron rest energy, ω=scattering angle.

$$\frac{E_{\text{src}} - E_d}{E_{\text{src}}} = \frac{1 - \cos(\omega)}{E_0}$$

Moral

- *If two photons from the same source hit the detector with the same energy, they have the same scattering angle.*

The Compton Effect

The Compton effect determines scattering angle

E_{src}=energy of *monochromatic* photons at the source,

E_d=measured energy of scattered photon at detector,

E_0=electron rest energy, ω=scattering angle.

$$\frac{E_{\text{src}} - E_d}{E_{\text{src}}} = \frac{1 - \cos(\omega)}{E_0}$$

Moral

- *If two photons from the same source hit the detector with the same energy, they have the same scattering angle.*
- *Therefore, they are on the same circle containing the source and detector!* *(if on the same side)*

Back scattered Compton Data are over *apples*

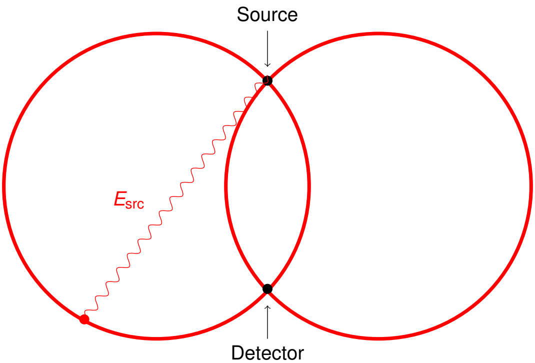

Photons leave the source with energy E_{src}.

Back scattered Compton Data are over *apples*

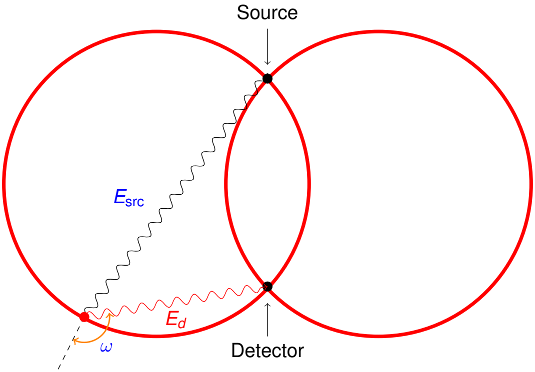

Photons leave the source with energy E_{src}.
Some will *back*scatter off the point with energy E_d measured at the detector.
E_d determines the scattering angle $\omega \in (\pi/2, \pi)$ and the apple part of the red circles (all points with scattering angle ω).

Back scattered Compton Data are over *apples*

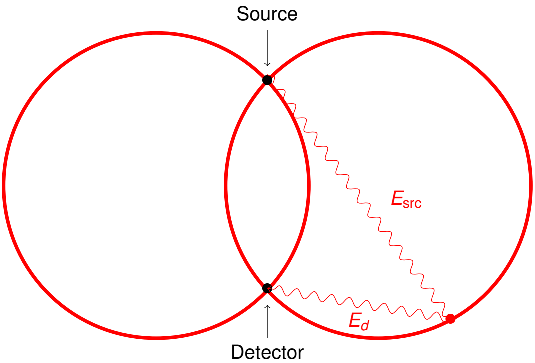

Photons leave the source with energy E_{src}.
Some will *back*scatter off the point with energy E_d measured at the detector.
E_d determines the scattering angle $\omega \in (\pi/2, \pi)$ and the apple part of the red circles (all points with scattering angle ω).
The same scattering occurs on the other circle.

Forward scattered Compton Data are over *lemons*

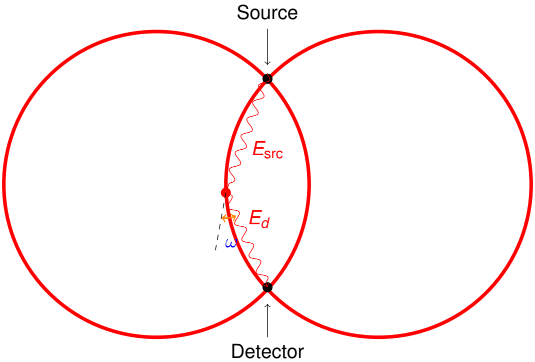

Photons leave the source with energy E_{src}.

Forward Scatter will occur on the lemon () part between the source and detector with scattering angle $\omega \in (0, \pi/2)$.

Previous works and dimensionality

1. Much of the literature considers these transforms over 3-D sets of lemons and apples [Webber, Q., Miller, Rigaud, Hahn, Webber, Holman, Cabeiro, et al.], [Arridge], etc.
2. [Rigaud, Hahn] With - 3-D data, artifacts observed due to incomplete data.
3. [Webber, Holman] With 3-D data, transform shown to violate the Bolker condition, and artifacts are induced by a flowout. Invisible singularities near the center due to limited energy resolution.
4. [Cabeiro, et al.] shows artifacts in simulated reconstructions.

Tufts UNIVERSITY

Previous works and dimensionality

1. Much of the literature considers these transforms over 3-D sets of lemons and apples [Webber, Q., Miller, Rigaud, Hahn, Webber, Holman, Cabeiro, et al.], [Arridge], etc.
2. [Rigaud, Hahn] With - 3-D data, artifacts observed due to incomplete data.
3. [Webber, Holman] With 3-D data, transform shown to violate the Bolker condition, and artifacts are induced by a flowout. Invisible singularities near the center due to limited energy resolution.
4. [Cabeiro, et al.] shows artifacts in simulated reconstructions.

Common theme: these authors analyze artifacts for various three-dimensional data sets.

The parametrization

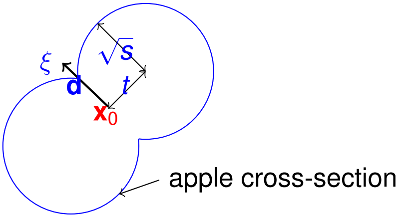

- $\mathbf{x}_0$ is the center of the spindle torus, $\mathbf{x}_T = \mathbf{x} - \mathbf{x}_0$.

The parametrization

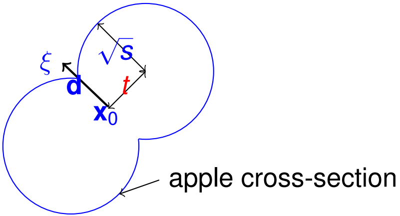

- $\mathbf{x}_0$ is the center of the spindle torus, $\mathbf{x}_T = \mathbf{x} - \mathbf{x}_0$.
- $t =$ the distance between the center of the torus and center of the generating circle.

The parametrization

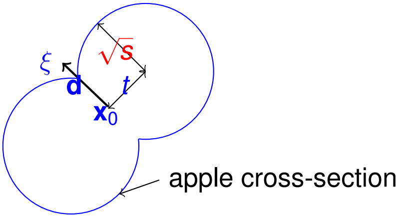

- $\mathbf{x}_0$ is the center of the spindle torus, $\mathbf{x}_T = \mathbf{x} - \mathbf{x}_0$.
- $t =$ the distance between the center of the torus and center of the generating circle.
- $s > t^2$ and $\sqrt{s}$ is the radius of the generating circle.

The parametrization

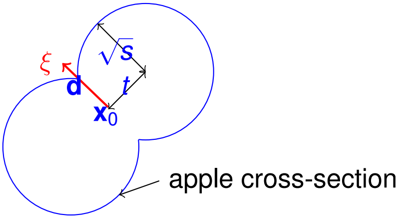

- $\mathbf{x}_0$ is the center of the spindle torus, $\mathbf{x}_T = \mathbf{x} - \mathbf{x}_0$.
- $t =$ the distance between the center of the torus and center of the generating circle.
- $s > t^2$ and $\sqrt{s}$ is the radius of the generating circle.
- $\xi \in S^2$ is parallel the axis of the spindle torus

The parametrization

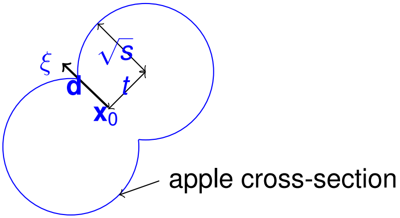

- $\mathbf{x}_0$ is the center of the spindle torus, $\mathbf{x}_T = \mathbf{x} - \mathbf{x}_0$.
- $t =$ the distance between the center of the torus and center of the generating circle.
- $s > t^2$ and $\sqrt{s}$ is the radius of the generating circle.
- $\xi \in S^2$ is parallel the axis of the spindle torus

$$\Psi_j(s, t, \mathbf{x}_0, \xi; \mathbf{x}) = \left(\|\mathbf{x}_T - \langle \mathbf{x}_T, \xi\rangle\xi\| + (-1)^j t\right)^2 + \langle \mathbf{x}_T, \xi\rangle^2 - s.$$

$\Psi_j = 0$ is the defining equation of the apple ($j = 1$) and lemon ($j = 2$) surfaces.

Some example surfaces

Here are some 2-D cross-sections of apples and lemons with the defining equations highlighted.

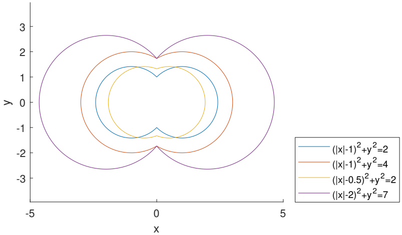

Apples ($j = 1$)

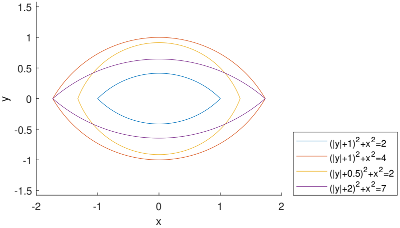

Lemons ($j = 2$)

(x, y) plane cross-sections of the apple and lemon parts of a spindle torus when $\xi = (0, 1)$ (left) and $\xi = (1, 0)$ (right), $\mathbf{x}_0 = \mathbf{0}$, and s and t vary between $\frac{1}{2}$ and 7.

Our generalized Radon transform

$f \in L^2_c(B)$, integrate over apple ($j=1$) and lemon ($j=2$) surfaces:

$$\mathcal{R}_j f(s,t,\mathbf{x}_0,\xi) = \int_X \|\nabla_{\mathbf{x}} \Psi_j\| \, \delta\left(\Psi_j(s,t,\mathbf{x}_0,\xi;\mathbf{x})\right) f(\mathbf{x}) \mathrm{d}\mathbf{x}$$

Our generalized Radon transform

$f \in L^2_c(B)$, integrate over apple ($j = 1$) and lemon ($j = 2$) surfaces:

$$\mathcal{R}_j f(s, t, \mathbf{x}_0, \xi) = \int_X \|\nabla_{\mathbf{x}} \Psi_j\| \, \delta\left(\Psi_j(s, t, \mathbf{x}_0, \xi; \mathbf{x})\right) f(\mathbf{x}) \mathrm{d}\mathbf{x}$$
$$= \frac{1}{2\pi} \int_{-\infty}^{\infty} \int_X \|\nabla_{\mathbf{x}} \Psi_j\| \, e^{i\sigma \Psi_j(s,t,\mathbf{x}_0,\xi;\mathbf{x})} f(\mathbf{x}) \mathrm{d}\mathbf{x} \mathrm{d}\sigma,$$

using $\frac{1}{2\pi} \int_{-\infty}^{\infty} e^{i\sigma r} \, \mathrm{d}\sigma = \delta(r)$.

Our generalized Radon transform

$f \in L_c^2(B)$, integrate over apple ($j = 1$) and lemon ($j = 2$) surfaces:

$$\begin{aligned}\mathcal{R}_j f(s, t, \mathbf{x}_0, \xi) &= \int_X \|\nabla_{\mathbf{x}} \Psi_j\| \, \delta\left(\Psi_j(s, t, \mathbf{x}_0, \xi; \mathbf{x})\right) f(\mathbf{x}) \mathrm{d}\mathbf{x} \\ &= \frac{1}{2\pi} \int_{-\infty}^{\infty} \int_X \|\nabla_{\mathbf{x}} \Psi_j\| \, e^{i\sigma \Psi_j(s,t,\mathbf{x}_0,\xi;\mathbf{x})} f(\mathbf{x}) \mathrm{d}\mathbf{x} \mathrm{d}\sigma,\end{aligned}$$

using $\frac{1}{2\pi}\int_{-\infty}^{\infty} e^{i\sigma r}\, \mathrm{d}\sigma = \delta(r)$.

Apple transform: $\mathcal{A}f = \mathcal{R}_1 f$

Lemon transform: $\mathcal{L}f = \mathcal{R}_2 f$

Our generalized Radon transform

$f \in L^2_c(B)$, integrate over apple ($j = 1$) and lemon ($j = 2$) surfaces:

$$\begin{aligned}\mathcal{R}_j f(s,t,\mathbf{x}_0,\xi) &= \int_X \|\nabla_{\mathbf{x}}\Psi_j\|\,\delta\left(\Psi_j(s,t,\mathbf{x}_0,\xi;\mathbf{x})\right) f(\mathbf{x})\mathrm{d}\mathbf{x} \\ &= \frac{1}{2\pi}\int_{-\infty}^{\infty}\int_X \|\nabla_{\mathbf{x}}\Psi_j\|\, e^{i\sigma\Psi_j(s,t,\mathbf{x}_0,\xi;\mathbf{x})} f(\mathbf{x})\mathrm{d}\mathbf{x}\mathrm{d}\sigma,\end{aligned}$$

using $\frac{1}{2\pi}\int_{-\infty}^{\infty} e^{i\sigma r}\,\mathrm{d}\sigma = \delta(r)$.

Apple transform: $\mathcal{A}f = \mathcal{R}_1 f$

Lemon transform: $\mathcal{L}f = \mathcal{R}_2 f$

Let $\overline{B}$ be the closed unit ball. The domain of $\mathcal{R}_j f$ is defined

$$\begin{aligned}Y =&\{(s,t,\mathbf{x}_0,\xi) \in \mathbb{R}^2 \times \mathbb{R}^3 \times S^2 \\ &: s > t^2, \{\mathbf{x}_0 \pm \sqrt{s-t^2}\xi\} \cap \overline{B} = \varnothing\},\end{aligned}.$$

Y describes the set of apples and lemons who's singular points (source and receiver) do not intersect $\overline{B}$.

Main theorem

Theorem (Webber, Q. *Inverse Problems* 38(2022))
The apple and lemon transforms $R_j : L^2_c(B) \to L^2_{loc}(Y)$ *are elliptic FIO order* -2.

Main theorem

Theorem (Webber, Q. *Inverse Problems* 38(2022))

The apple and lemon transforms $R_j : L^2_c(B) \to L^2_{loc}(Y)$ *are elliptic FIO order* -2.
The left projections $\Pi_L^{(1)}, \Pi_L^{(2)}$ *of* $\mathcal{A}, \mathcal{L}$*, respectively, are injective immersions, i.e.,* $\mathcal{A}, \mathcal{L}$ *satisfy the Bolker condition.*

Main theorem

Theorem (Webber, Q. *Inverse Problems* **38**(2022))

The apple and lemon transforms $R_j : L^2_c(B) \to L^2_{loc}(Y)$ *are elliptic FIO order* -2.
The left projections $\Pi_L^{(1)}, \Pi_L^{(2)}$ *of* $\mathcal{A}, \mathcal{L}$*, respectively, are injective immersions, i.e.,* $\mathcal{A}, \mathcal{L}$ *satisfy the Bolker condition.*

Key point: With full seven-dimensional data, the lemon and apple transforms satisfy the Bolker condition.

Main theorem

Theorem (Webber, Q. *Inverse Problems* 38(2022))

The apple and lemon transforms $R_j : L^2_c(B) \to L^2_{loc}(Y)$ are elliptic FIO order -2.

The left projections $\Pi^{(1)}_L, \Pi^{(2)}_L$ of $\mathcal{A}, \mathcal{L}$, respectively, are injective immersions, i.e., $\mathcal{A}, \mathcal{L}$ satisfy the Bolker condition.

Key point: With full seven-dimensional data, the lemon and apple transforms satisfy the Bolker condition.

- Thus, there are no artifacts in backprojection type reconstructions from seven-dimensional lemon or apple integral data, $\mathcal{K} = R^*_j D\varphi R_j f$ where φ is smooth (i.e., $\mathcal{K}$ is a ΨDO).

Main theorem

Theorem (Webber, Q. *Inverse Problems* **38**(2022))

The apple and lemon transforms $R_j : L^2_c(B) \to L^2_{loc}(Y)$ *are elliptic FIO order* -2.
The left projections $\Pi_L^{(1)}, \Pi_L^{(2)}$ *of* $\mathcal{A}, \mathcal{L}$*, respectively, are injective immersions, i.e.,* $\mathcal{A}, \mathcal{L}$ *satisfy the Bolker condition.*

Key point: With full seven-dimensional data, the lemon and apple transforms satisfy the Bolker condition.

- Thus, there are no artifacts in backprojection type reconstructions from seven-dimensional lemon or apple integral data, $\mathcal{K} = R_j^* D\varphi R_j f$ where φ is smooth (i.e., $\mathcal{K}$ is a ΨDO).
- Also, we show there are no invisible singularities on B with data over all Y.

Proof outline:

1. Calculate the canonical relation, $\mathcal{C}_j$ of R_j and choose good coordinates.

$$R = R(\alpha,\beta) = \begin{pmatrix} \cos\alpha & -\sin\alpha & 0 \\ \sin\alpha & \cos\alpha & 0 \\ 0 & 0 & 1 \end{pmatrix} \begin{pmatrix} 1 & 0 & 0 \\ 0 & \cos\beta & -\sin\beta \\ 0 & \sin\beta & \cos\beta \end{pmatrix}, \quad \xi = R\mathbf{e}_3.$$

Proof outline:

1. Calculate the canonical relation, $\mathcal{C}_j$ of R_j and choose good coordinates.
$$R = R(\alpha,\beta) = \begin{pmatrix} \cos\alpha & -\sin\alpha & 0 \\ \sin\alpha & \cos\alpha & 0 \\ 0 & 0 & 1 \end{pmatrix} \begin{pmatrix} 1 & 0 & 0 \\ 0 & \cos\beta & -\sin\beta \\ 0 & \sin\beta & \cos\beta \end{pmatrix}, \quad \xi = R\mathbf{e}_3.$$
2. Show the symbol of $\mathcal{R}_j$ is smooth and never zero (singular points on our spindle tori don't meet B).

Proof outline:

1. Calculate the canonical relation, $\mathcal{C}_j$ of R_j and choose good coordinates.
$$R = R(\alpha,\beta) = \begin{pmatrix} \cos\alpha & -\sin\alpha & 0 \\ \sin\alpha & \cos\alpha & 0 \\ 0 & 0 & 1 \end{pmatrix} \begin{pmatrix} 1 & 0 & 0 \\ 0 & \cos\beta & -\sin\beta \\ 0 & \sin\beta & \cos\beta \end{pmatrix}, \quad \xi = R\mathbf{e}_3.$$
2. Show the symbol of $\mathcal{R}_j$ is smooth and never zero (singular points on our spindle tori don't meet B).
3. Recall *Sylvester's Determinant Theorem (SDT)*:
$A \in \mathbb{R}^{m\times n}$, $B \in \mathbb{R}^{n\times m}$: $\det\left(I_{m\times m} + AB\right) = \det\left(I_{n\times n} + BA\right).$

Proof outline:

1. Calculate the canonical relation, $\mathcal{C}_j$ of R_j and choose good coordinates.
$$R = R(\alpha,\beta) = \begin{pmatrix} \cos\alpha & -\sin\alpha & 0 \\ \sin\alpha & \cos\alpha & 0 \\ 0 & 0 & 1 \end{pmatrix} \begin{pmatrix} 1 & 0 & 0 \\ 0 & \cos\beta & -\sin\beta \\ 0 & \sin\beta & \cos\beta \end{pmatrix}, \quad \xi = R\mathbf{e}_3.$$
2. Show the symbol of $\mathcal{R}_j$ is smooth and never zero (singular points on our spindle tori don't meet B).
3. Recall *Sylvester's Determinant Theorem (SDT)*:
$A \in \mathbb{R}^{m\times n}$, $B \in \mathbb{R}^{n\times m}$: $\det\left(I_{m\times m} + AB\right) = \det\left(I_{n\times n} + BA\right).$
4. Show that the phase function is nondegenerate.

Proof outline:

1. Calculate the canonical relation, $\mathcal{C}_j$ of R_j and choose good coordinates.
$$R = R(\alpha, \beta) = \begin{pmatrix} \cos\alpha & -\sin\alpha & 0 \\ \sin\alpha & \cos\alpha & 0 \\ 0 & 0 & 1 \end{pmatrix} \begin{pmatrix} 1 & 0 & 0 \\ 0 & \cos\beta & -\sin\beta \\ 0 & \sin\beta & \cos\beta \end{pmatrix}, \quad \xi = R\mathbf{e}_3.$$
2. Show the symbol of $\mathcal{R}_j$ is smooth and never zero (singular points on our spindle tori don't meet B).
3. Recall *Sylvester's Determinant Theorem (SDT)*:
$A \in \mathbb{R}^{m\times n}$, $B \in \mathbb{R}^{n\times m}$: $\det\left(I_{m\times m} + AB\right) = \det\left(I_{n\times n} + BA\right).$
4. Show that the phase function is nondegenerate.
5. Show that $\Pi_L^{(j)}$ is an injective immersion (SDT).

Proof outline:

1. Calculate the canonical relation, $\mathcal{C}_j$ of R_j and choose good coordinates.
$$R = R(\alpha,\beta) = \begin{pmatrix} \cos\alpha & -\sin\alpha & 0 \\ \sin\alpha & \cos\alpha & 0 \\ 0 & 0 & 1 \end{pmatrix} \begin{pmatrix} 1 & 0 & 0 \\ 0 & \cos\beta & -\sin\beta \\ 0 & \sin\beta & \cos\beta \end{pmatrix}, \quad \xi = R\mathbf{e}_3.$$
2. Show the symbol of $\mathcal{R}_j$ is smooth and never zero (singular points on our spindle tori don't meet B).
3. Recall *Sylvester's Determinant Theorem (SDT)*:
$A \in \mathbb{R}^{m\times n}$, $B \in \mathbb{R}^{n\times m}$: $\det\left(I_{m\times m} + AB\right) = \det\left(I_{n\times n} + BA\right)$.
4. Show that the phase function is nondegenerate.
5. Show that $\Pi_L^{(j)}$ is an injective immersion (SDT).
Each of these calculations has an expression:
$$\det\left(I_{3\times 3} - \frac{t}{g}\left(r_1^T, r_2^T\right)\begin{pmatrix} r_1 \\ r_2 \end{pmatrix}\right) = \det\left(I_{2\times 2} - \frac{t}{g}\begin{pmatrix} r_1 \\ r_2 \end{pmatrix}\left(r_1^T, r_2^T\right)\right)$$
where r_1 and r_2 are the first two rows of R^T, $g = \|\mathbf{x}_T - \langle \mathbf{x}_T, \xi\rangle\xi\|$.

A five-dimensional set of spindle tori

Corollary ([Webber, Q.])

Let $\xi_0 \in S^2$ *be fixed. Then the Radon transform over lemons with axis parallel* ξ_0

$$\mathcal{L}_T f(s, t, \mathbf{x}_0) = \mathcal{L} f(s, t, \mathbf{x}_0, \xi_0)$$

satisfies the Bolker condition on domain $\mathcal{E}'(B)$.

Tufts UNIVERSITY

A five-dimensional set of spindle tori

Corollary ([Webber, Q.])

Let $\xi_0 \in S^2$ *be fixed. Then the Radon transform over lemons with axis parallel* ξ_0

$$\mathcal{L}_T f(s, t, \mathbf{x}_0) = \mathcal{L} f(s, t, \mathbf{x}_0, \xi_0)$$

satisfies the Bolker condition on domain $\mathcal{E}'(B)$*.*
The apple transform with ξ_0 *fixed*

$$\mathcal{A}_T f(s, t, \mathbf{x}_0) = \mathcal{A} f(s, t, \mathbf{x}_0, \xi_0),$$

however, does not satisfy the Bolker condition.

A five-dimensional set of spindle tori

Corollary ([Webber, Q.])

Let $\xi_0 \in S^2$ be fixed. Then the Radon transform over lemons with axis parallel ξ_0

$$\mathcal{L}_T f(s,t,\mathbf{x}_0) = \mathcal{L} f(s,t,\mathbf{x}_0,\xi_0)$$

satisfies the Bolker condition on domain $\mathcal{E}'(B)$.
The apple transform with ξ_0 fixed

$$\mathcal{A}_T f(s,t,\mathbf{x}_0) = \mathcal{A} f(s,t,\mathbf{x}_0,\xi_0),$$

however, does not satisfy the Bolker condition.

1. *Specifics:* The left projection of $\mathcal{A}_T$ has Jacobian which drops rank above the cylinder $t = \|\mathbf{x}_T - \langle \mathbf{x}_T, \xi_0 \rangle \xi_0\|$.

A five-dimensional set of spindle tori

Corollary ([Webber, Q.])

Let $\xi_0 \in S^2$ *be fixed. Then the Radon transform over lemons with axis parallel* ξ_0

$$\mathcal{L}_T f(s, t, \mathbf{x}_0) = \mathcal{L} f(s, t, \mathbf{x}_0, \xi_0)$$

satisfies the Bolker condition on domain $\mathcal{E}'(B)$*.*
The apple transform with ξ_0 *fixed*

$$\mathcal{A}_T f(s, t, \mathbf{x}_0) = \mathcal{A} f(s, t, \mathbf{x}_0, \xi_0),$$

however, does not satisfy the Bolker condition.

1. *Specifics:* The left projection of $\mathcal{A}_T$ has Jacobian which drops rank above the cylinder $t = \|\mathbf{x}_T - \langle \mathbf{x}_T, \xi_0 \rangle \xi_0\|$.

   Therefore, artifacts can appear in the reconstruction along rings which are the intersections of apples and the cylinder of radius t with the same axis of revolution.

2-D cross-section of a spindle torus with this cylinder.

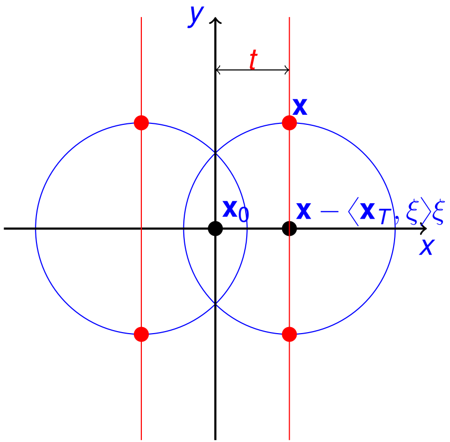

The cylinder intersects the apple along rings at the top and bottom of the apple. The red points on the apple are where Π_L drops rank.

2-D cross-section of a spindle torus with this cylinder.

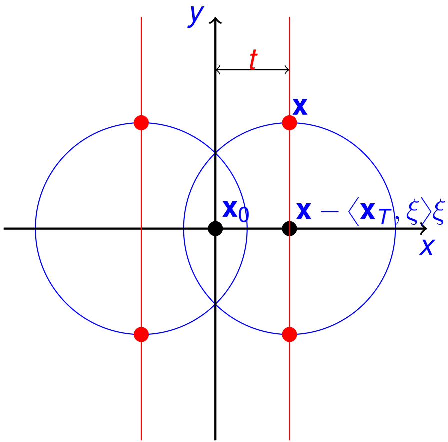

The cylinder intersects the apple along rings at the top and bottom of the apple. The red points on the apple are where Π_L drops rank.

The cylinder never intersects the lemon, so Bolker holds for $\mathcal{L}_T$.

A 3-dimensional geometry from luggage testing

We consider the practical geometry where the sources are on the plane $z = 1$ and the detectors are on the plane $z = -1$ [Webber, Q., Miller] .

A 3-dimensional geometry from luggage testing

We consider the practical geometry where the sources are on the plane $z = 1$ and the detectors are on the plane $z = -1$ [Webber, Q., Miller] . This gives parameters:

- $\mathbf{x}_0 \in \mathbb{R}^2$: $(\mathbf{x}_0, 0)$ is the center of the spindle torus
- $t \in (0, \infty)$: the distance from $(\mathbf{x}_0, 0)$ to the center of the circle generating the torus. So, $s = t^2 + 1$

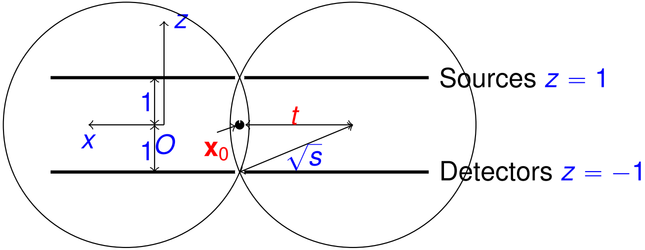

A 3-dimensional geometry from luggage testing

We consider the practical geometry where the sources are on the plane $z = 1$ and the detectors are on the plane $z = -1$ [Webber, Q., Miller] . This gives parameters:

- $\mathbf{x}_0 \in \mathbb{R}^2$: $(\mathbf{x}_0, 0)$ is the center of the spindle torus
- $t \in (0, \infty)$: the distance from $(\mathbf{x}_0, 0)$ to the center of the circle generating the torus. So, $s = t^2 + 1$
- The detector is directly below the source and they move together.

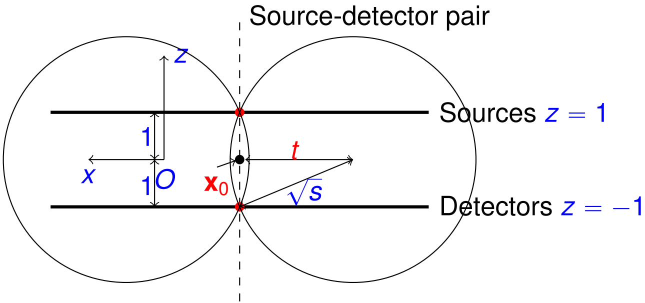

The transforms for luggage testing

$$\mathcal{A}_0 f_1(t, \mathbf{x}_0) = \mathcal{A} f\left(t^2 + 1, t, (\mathbf{x}_0, 0)^T, \mathbf{e}_3)\right)$$

1. $\mathcal{A}_0$ is an FIO for compactly supported distributions on $\{z > 1\}$ (above the detector array)–or below.

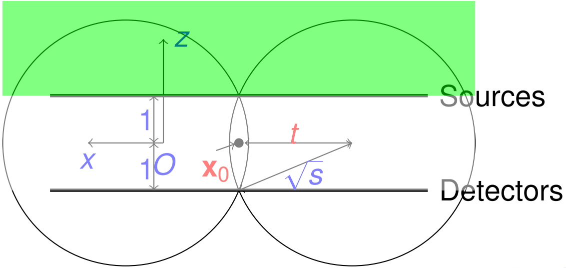

The transforms for luggage testing

$$\mathcal{A}_0 f_1(t, \mathbf{x}_0) = \mathcal{A}f\left(t^2+1, t, (\mathbf{x}_0, 0)^T, \mathbf{e}_3\right)$$

and

$$\mathcal{L}_0 f(t, \mathbf{x}_0) = \mathcal{L}f\left(t^2+1, t, (x_0, y_0, 0)^T, \mathbf{e}_3\right).$$

1. $\mathcal{A}_0$ is an FIO for compactly supported distributions on $\{z > 1\}$ (above the detector array)–or below.
2. $\mathcal{L}_0$ is an FIO for compactly supported distributions on $\{-1 < z < 1\}$ (in-between the source and detector array).

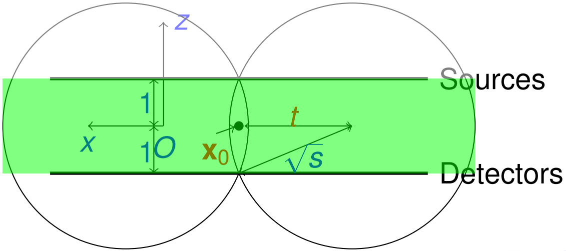

Theorem

- *The lemon transform $\mathcal{L}_0$ satisfies the Bolker condition for distributions in $\mathcal{E}'(\{0 < z < 1\})$.*

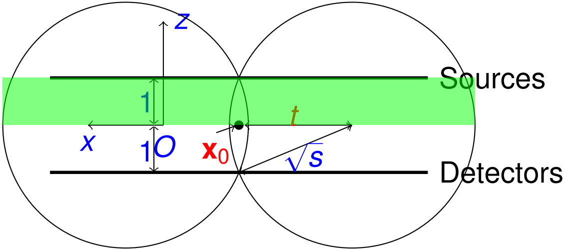

Theorem

- *The lemon transform $\mathcal{L}_0$ satisfies the Bolker condition for distributions in $\mathcal{E}'(\{0 < z < 1\})$.*

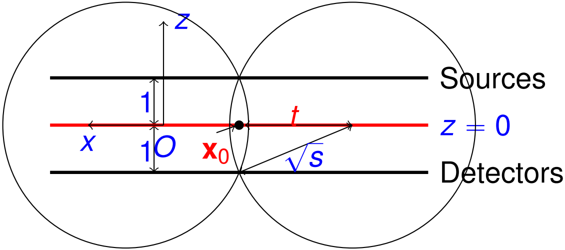

On $\{-1 < z < 1\}$, artifacts occur at mirror points–reflections in $z = 0$

Theorem

- *The apple transform $\mathcal{A}_0$ satisfies Bolker for distributions supported in the region above the hyperboloid*

$$H(\mathbf{x}_0) = \{(x, y, z) : z^2 - 1 = (x - x_0)^2 + (y - y_0)^2\}$$

Π_L drops rank at the red points where the apple intersects $H(\mathbf{x}_0)$.

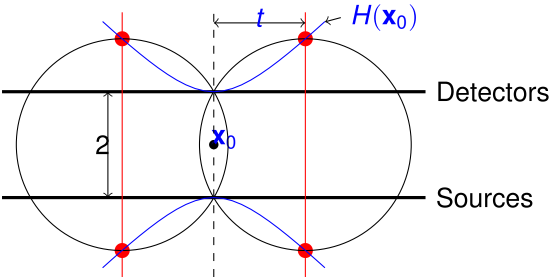

Theorem

- *The apple transform $\mathcal{A}_0$ satisfies Bolker for distributions supported in the region above the hyperboloid*

$$H(\mathbf{x}_0) = \left\{(x, y, z) : z^2 - 1 = (x - x_0)^2 + (y - y_0)^2\right\}$$

Π_L drops rank at the red points where the apple intersects $H(\mathbf{x}_0)$.

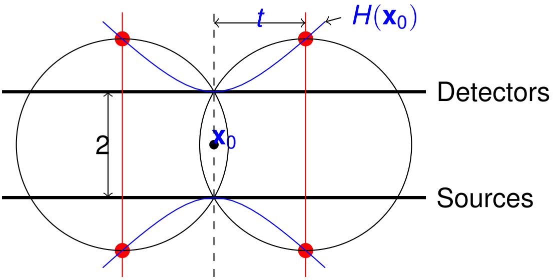

Warning: This region where Bolker holds depends on $\mathbf{x}_0$!

Artifact Reduction

Put $\mathrm{supp}(f)$ above $z = 1 + \epsilon$ and restrict the source cone-beam angle to only illuminate $\mathrm{supp}(f)$ above $H(\mathbf{x}_0)$

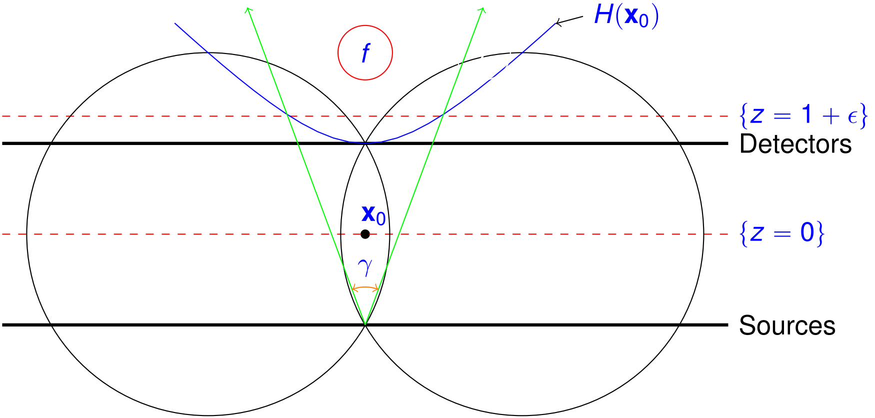

Artifact Reduction

Put $\operatorname{supp}(f)$ above $z = 1 + \epsilon$ and restrict the source cone-beam angle to only illuminate $\operatorname{supp}(f)$ above $H(\mathbf{x}_0)$

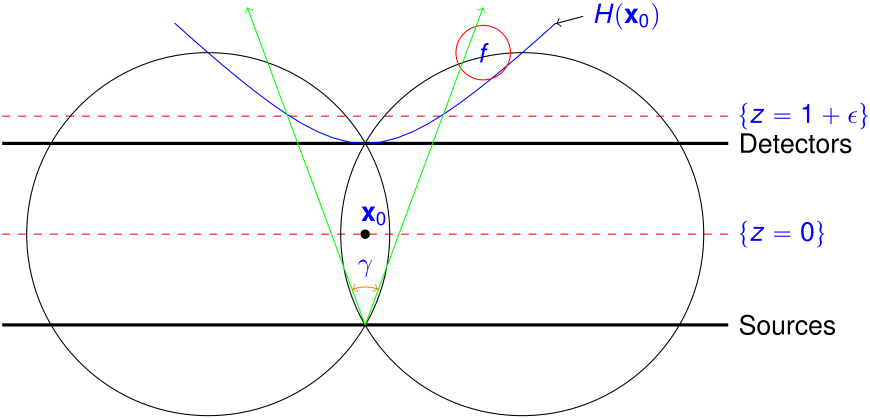

As the source and detector pairs move, only the part of $\operatorname{supp}(f)$ above $H(\mathbf{x}_0)$ is illuminated.

Summary

- We introduced two new seven-dimensional generalized Radon transforms, $\mathcal{A}$ and $\mathcal{L}$.

Summary

- We introduced two new seven-dimensional generalized Radon transforms, $\mathcal{A}$ and $\mathcal{L}$.
- We proved for the full 7-dim problem that $\mathcal{A}$ and $\mathcal{L}$ satisfy Bolker.

Summary

- We introduced two new seven-dimensional generalized Radon transforms, $\mathcal{A}$ and $\mathcal{L}$.
- We proved for the full 7-dim problem that $\mathcal{A}$ and $\mathcal{L}$ satisfy Bolker.
- We analyzed lower dimensional cases, including a practical geometry for luggage testing.

Summary

- We introduced two new seven-dimensional generalized Radon transforms, $\mathcal{A}$ and $\mathcal{L}$.
- We proved for the full 7-dim problem that $\mathcal{A}$ and $\mathcal{L}$ satisfy Bolker.
- We analyzed lower dimensional cases, including a practical geometry for luggage testing.
- We discovered artifacts and suggested ways to remove artifacts with machine design.

Summary

- We introduced two new seven-dimensional generalized Radon transforms, $\mathcal{A}$ and $\mathcal{L}$.
- We proved for the full 7-dim problem that $\mathcal{A}$ and $\mathcal{L}$ satisfy Bolker.
- We analyzed lower dimensional cases, including a practical geometry for luggage testing.
- We discovered artifacts and suggested ways to remove artifacts with machine design.
- *See:* [Microlocal properties of seven-dimensional lemon and apple Radon transforms with applications in Compton scattering tomography. Inverse Problems **38**(2022) 064001].

Summary

- We introduced two new seven-dimensional generalized Radon transforms, $\mathcal{A}$ and $\mathcal{L}$.
- We proved for the full 7-dim problem that $\mathcal{A}$ and $\mathcal{L}$ satisfy Bolker.
- We analyzed lower dimensional cases, including a practical geometry for luggage testing.
- We discovered artifacts and suggested ways to remove artifacts with machine design.
- *See:* [Microlocal properties of seven-dimensional lemon and apple Radon transforms with applications in Compton scattering tomography. Inverse Problems **38**(2022) 064001].

Thanks for listening!

References

- J. Webber, E.T. Quinto, and E.L. Miller. “A joint reconstruction and lambda tomography regularization technique for energy-resolved X-ray imaging” Inverse Problems **36** (2020) 074002 (32pp).
- J. Webber and S. Holman. "Microlocal analysis of a spindle transform." *Inverse Problems and Imaging* **2**(2019), 231-261.
- J. Cebeiro, C. Tarpau, M.A. Morvidone, D. Rubio, and M.K. Nguyen. "On a three-dimensional Compton scattering tomography system with fixed source." Inverse Problems **37**, no. 5 (2021): 054001.
- G. Rigaud and B.N. Hahn. "Reconstruction algorithm for 3D Compton scattering imaging with incomplete data." Inverse Problems in Science and Engineering **29**, no. 7 (2021): 967-989.
- J. Webber and E.T. Quinto. "Microlocal properties of seven-dimensional lemon and apple Radon transforms with applications in Compton scattering tomography." Inverse Problems **38**(2022) 064001.